The Blue Marble Next Generation - A true color earth dataset including seasonal dynamics from MODIS

Reto Stöckli[*], Eric Vermote[†], Nazmi Saleous[‡], Robert Simmon[§] and David Herring[¶]

June 28, 2005

Contents

[*]Corresponding author: Reto Stöckli, IACETH, Winterthurerstrasse 190, 8057 Zürich, Switzerland. e-mail: rstockli@climate.gsfc.nasa.gov, phone: +41 44 635 5209. Affiliations: NASA Earth Observatory and ETH Institute for Atmospheric and Climate Science

[†]Department of Geography, University of Maryland, College Park, MD 20742, USA

[‡]Department of Geography, University of Maryland, College Park, MD 20742, USA

[§]NASA Earth Observatory, Mail Code 613.2, Goddard Space Flight Center, Greenbelt, MD 20771, USA

[¶]NASA Earth Observatory, Mail Code 613.2, Goddard Space Flight Center, Greenbelt, MD 20771, USA

Abstract

Satellite remote sensors provide the science community with high quality datasets to better understand and monitor Earth's environment and climate system. When used in education, these datasets allow visual exploration of the planet at moderately high spatial and temporal resolutions. However, native data file formats and file sizes are not well suited for public distribution. To help circumvent these issues, the Blue Marble Next Generation (BMNG) is a new series of 12 monthly cloud-free, global-scale images. We created the BMNG using NASA Terra MODerate resolution Imaging Spectroradiometer (MODIS) science data collected in 2004. We temporally adjusted the data using a discrete Fourier technique. This correction method removed cloud disturbances, but snow reflectance remains a significant challenge. The BMNG visualizes seasonal changes of the land surface (spring greening, snowmelt, drought, etc.) as true-color images and Normalized Difference Vegetation Index (NDVI) maps in monthly steps at 500-m spatial resolution. The images are available at no cost from NASA.

1 Introduction

Space exploration changed our visual perception of planet Earth. In 1950s, satellites revolutionized weather forecasting when they began beaming home television images of cloud patterns. Astronaut photography in the early 1970s showed us the whole Earth"disk" for the first time in true-color – the so-called "Blue Marble" (Figure 1 left). Since 1972, satellite sensors have been acquiring atmosphere, land, ice and ocean data with increasing spectral, spatial and temporal resolution. Satellite remote sensing systems like NASAs Earth Observing System (EOS) help us to understand and monitor Earth's physical, chemical, and biological processes [Wielicki et al., 1995, Kaufman et al., 1998, Running et al., 1999].

Figure 1: Earth views: Apollo 17 astronaut photograph (left, 1972), Blue Marble false color composite (center, 2000), MODIS Blue Marble true color composite (right, 2002)

The false-color Earth image [Stöckli et al., 2000] shown in Figure 1 (center) was created from Advanced Very High Resolution Radiometer (AVHRR), Geostationary Operational Environmental Satellite (GOES-8), and Sea-viewing Wide Field-of-view Sensor (SeaWiFS) data. Named the "Blue Marble", that image was created for public outreach and it demonstrated the high value of such visualizations. New sensors like MODIS, aboard NASAs Terra and Aqua satellites, observe and measure a wide range of geophysical parameters. In 2002 we created the true-color Earth image in Figure 1 (right) using MODIS land, ocean, ice and atmosphere science products [Stöckli et al., 2002]. This image has been widely used in museums, print media, TV documentaries, in movies, by mapping agencies, and in NASA's public communications about its missions and research initiatives.

The success of the Blue Marble imagery motivated us to continue the project. The BMNG is a cloud-free true-color dataset at 500-m spatial resolution and monthly temporal resolution. Whereas cloud-free Earth imagery is commercially available (e.g., The Living Earth Inc., WorldSat International Inc.), the BMNG aims at providing freely available data from the Earth surface in true color, derived from scientific data as a value-added product. Although the spatial resolution of the BMNG is comparable to other datasets, seasonal variations with monthly time-steps have not been shown before in seamless true-color composites. A visualization of seasonal variations (snowfall, droughts, wet seasons, spring greening, etc.) has good potential to enhance education. Furthermore, the BMNG can help to increase public understanding (and therefore acceptance) of satellite missions and awareness of causes and effects of changes in Earth's climate system.

The creation of seamless cloud-free spatial and temporal composites of Earth's surface is, however, not a trivial task. It is dependent on sophisticated atmospheric corrections [Vermote et al., 1997] and cloud screening. Even then, cloudy pixels, missing time periods, and processing artifacts [Los et al., 2000], can disturb satellite derived data. Temporal compositing based on empirical filters (Maximum value composite, Holben [1986]) can be used to remove such irregularities. An ecosystem-dependent spatio-temporal interpolation has been successfully applied to MODIS albedo data by Moody et al. [2005]. For the BMNG dataset, we used a temporal adjustment based on discrete Fourier series. This method is well suited to creating consistent NDVI time-series images from AVHRR data [Los et al., 2000, Stöckli and Vidale, 2004], but had not been applied to true-color imagery until now.

The next sections describe the science behind the BMNG imagery and provide examples, showing the performance of the method we used.

2 Methods

We used a temporal correction based on discrete Fourier series to create monthly land surface reflectance composites from MOD09A1 (TERRA satellite) data. This method assumes that the snow-free land surface changes on a seasonal timescale with a yearly periodicity [Moulin et al., 1997]. Second order Fourier series allow to model this temporal pattern, which was successfully demonstrated by Los et al. [2000] and Stöckli and Vidale [2004]. Fourier series can be fitted to a disturbed or incomplete measurement time series and still represent the seasonal changes very well, while ignoring short-term disturbances. Some artificial landscapes, like cropfields, can have more than one growing cycle during a year. We used third order Fourier series to account for this pattern when we had enough data to fit such a curve. Some areas do not show substantial seasonal change (such as lakes, ocean, and permanently snow-covered areas) nor do they have sufficient temporal coverage (tropical rainforests) due to persistent cloud cover or aerosols. For those areas we used weighted averaging to temporally composite their reflectance values. First, we quality checked individual MODIS bands, followed by a snow-free Fourier adjustment. As a last step, we added the reflectance values for snow-covered areas to the snow-free dataset and then transformed the data into true-color imagery and NDVI maps.

2.1 Data

The BMNG is based on MODIS land surface reflectance data (MOD09, Justice et al. [2002]) – the reflectance that would be measured coming off the land surface if there were no atmosphere. This measure is calculated from MODIS top-of-atmosphere reflectances by applying corrections to remove the effect of gaseous absorption, molecules and aerosol scattering [Vermote et al., 1997]. In comparison to earlier satellite-derived surface reflectance products (e.g. from AVHRR; [James and Kalluri, 1994, Csiszar and Gutman, 1999]), the MODIS land surface reflectance is corrected for aerosols. This novel correction is important for the monthly BMNG dataset, since aerosol effects can remain in uncorrected datasets even after monthly temporal compositing periods [Vermote et al., 2002].
All MOD09 8-day composites (MOD09A1, Collection 4) from 2004 were used. Bands 1 (red), 2 (near-IR), 3 (blue) and 4 (green), the internal snow cover flag,

and the internal cloud mask at 500-m spatial resolution were quality screened through the use of the provided quality flags:

1. bands 1,2,3 and 4 extracted if quality assurance (QA) bits are ideal quality (sur_refl_qc_500m bits 0 and 1) and none of the bands have fill values
2. snow masked if the internal snow mask flagged (sur_refl_state_500m bit 12)
3. cloud masked if the internal cloud mask or the cloud shadow mask flagged (sur_refl_state_500m bits 2 and 10)
4. steps 1-3 only performed if the aerosol quality is high (sur_refl_state_500m bits 6 and 7)

We used a time-invariant land cover map where the surface reflectance product provided insufficient temporal information – specifically, the MODIS landcover dataset (MOD12Q1, year 2001, Collection 4, IGBP classification) derived through the use of a supervised classification methodology [Friedl et al., 2002].

2.2 Temporal snow-free correction

We applied a weighting scheme to all valid snow-free and cloud-free 8-day MOD09A1 reflectance values. This method eliminates MODIS cloud and snow mask failures. Contamination of snow and cloud pixels is problematic for fitting discrete Fourier series. The weights W_i are based on the standard deviation of reflectance values X_{i_b} between bands $b = 1 \ldots nb$, where $nb = 4$ is the number of bands. Large weights are given to pixels showing a high standard deviation (relative to their magnitude: e.g. dense green vegetation) and small weights are given to pixels, where all color values are in the similar range (e.g. clouds, snow);

$$W_i = \frac{1}{\bar{X}_i} \sqrt{\sum_{b=1}^{nb} (X_{i_b} - \bar{X}_i)^2} \tag{1}$$

where $i = 1 \ldots n$ and $n = 46$ is the number of 8-day reflectance composites per year. Using this scheme, non-vegetated areas such as deserts, salt lakes, and permanent snow receive a constant low weighting during the course of a year. Weights W_i are therefore normalized by their yearly mean value. The Fourier matrix

$$(F^T F)c = F^T W X \tag{2}$$

is solved for the Fourier coefficients c_{j_b} by use of singular value decomposition, where

$$F_i = W_i \left[\begin{array}{ccccccc} 1 & \cos\phi_i & \sin\phi_i & \cdots & \cos(m-1)\phi_i & \sin(m-1)\phi_i \end{array} \right] \tag{3}$$

is a matrix n x $(2m-1)$, $\phi_i = (2\pi i)/n$, and $j = 1 \ldots 2m-1$. m is the order of the resulting discrete Fourier series

$$Y_{i_b} = c_{1_b} + c_{2_b} \cos\phi_i + c_{3_b} \sin\phi_i + \ldots + c_{2m_b} \cos(m-1)\phi_i + c_{2m+1_b} \sin(m-1)\phi_i \tag{4}$$

and $m = 2$ when the longest gap in X is between 1-3 months and $m = 3$ when the longest gap is shorter than one month. Time-series with longer gaps (but with at least 3 valid reflectances) are linearly interpolated, only using values with $W_i > 0.5$. Monthly snow-free surface reflectances are created from Y_{i_b} by averaging. Water pixels (Discriminated by the MOD12Q1 land cover dataset) are averaged over the entire year, discarding values where $W_i < 1.0$.

Table 1: Scaling land surface reflectance to RGB space

Spline	RGB	Reflectance
1	0	0%
2	64	62.5%
3	191	94%
4	255	100%

2.3 Temporal correction of snow

Snowfall and snowmelt create rapid changes in surface reflectance, which is not in accordance with the assumptions made for use of second or third order discrete Fourier series. Snow is therefore added to the snow-free reflectances. Snow-flagged reflectances replace the monthly snow-free reflectances if at least half of the monthly 8-day composites are snow-flagged. Due to missing sunlight, high latitudes are subject to extended data dropouts in winter. We used a simple approximation for these areas. Snow reflectances are linearly interpolated between autumn and spring values.

2.4 Spatial gap filling

The above correction method fails for areas with less than three valid reflectances during a year. These are predominantly tropical rainforests (constant cloud cover), areas with excessive biomass burning (high aerosol loading) and deep ocean (no MOD09A1 reflectances). A spatial interpolation technique based on land cover classification is used in this case (in the following order):

1. Missing pixels are replaced by the mean (weighted by inverse distance) of surrounding corrected pixels of the same land cover class (MOD12Q1), using a radius of three pixels;

2. Missing pixels are replaced by the mean reflectance of all corrected pixels of the same land cover class (MOD12Q1);

3. Deep ocean pixels are replaced by an arbitrary ocean reflectance (bands 1=0.2%, 4=0.55% and 3=2%).

2.5 Scaling to RGB and NDVI space

Due to the high dynamic range of surface reflectance values, visualization of Earths landscapes presents a significant challenge. While dense vegetation shows a mean reflectance of 2-5% in the visible spectrum, snow and ice surfaces reflect more than 90% of the incoming radiation and appear very bright. For most visualization purposes, this large range of intensity creates problems. The BMNG images were therefore contrast enhanced, transforming the corrected bands 1, 4 and 3 into the RGB space [Tholey, 2000] by use of a cubic spline function (Table 1). We calculated monthly NDVI of all corrected land pixels as follows: NDVI =(band 2 - band 1)/(band 2 + band 1).

3 Results

Figure 2 shows a time-series of uncorrected and Fourier-adjusted reflectances. The Alpine mixed forest (a) has a long growing season. Visible reflectances are lower

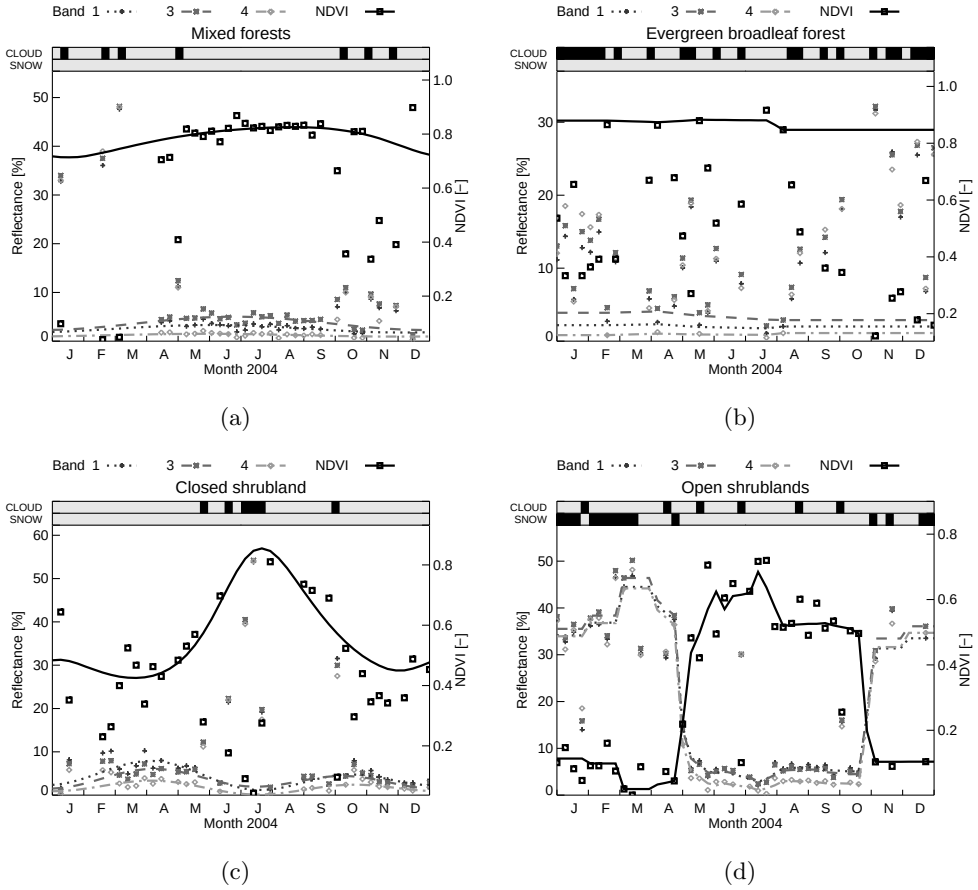

Figure 2: Yearly time-series of uncorrected (symbols) and Fourier-adjusted (lines) land surface reflectances / NDVI : a) Alpine mixed forest; b) tropical rainforest in Sumatra; c) shrubland in Tibetian plateau; d) shrubland in Utah, USA.

in winter (wet soil) than in summer. The NDVI is slightly lower in winter, when the deciduous part of vegetation has lost its leaves. The cloud flag (top of the graph) captures cloud-disturbed pixels, except for one (beginning of October), which receives a low weight in the Fourier adjustment process and is not included in the resulting time-series. Significantly heavier cloud contamination is seen in reflectances of a tropical rainforest in Sumatra (b). However, the situation there is not helpless since the cloud mask in combination with the weighting scheme we used allowed us to reconstruct the constantly high NDVI time-series and a low Albedo of 2-5% in the visible bands. NDVI slightly decreased after July during the dry season.

High-altitude vegetation like shrubs in the Tibetian plateau (c) only grows during a short period, being limited by temperature. Clouds obscure observations during the Monsoon season, but the short peak in NDVI has been reconstructed by the use of discrete Fourier series. Snow cover changes surface albedo from 10-50% within one 8-day period, as shown in a time-series over the western United States (d). The snow-free Fourier adjustment provides summer reflectance time-series, and snow is patched in winter based on snow flags. However, the beginning and end of snow cover is not clear. The MODIS snow flag shows snow from January to March and at the end of December, while observed reflectances suggest snow from January to April and during November and December. Discriminating snow

cover from the snow-free reflectances is one of the main problems in the BMNG algorithm. In areas with short periods of snowfall (e.g., snow storms), clouds and snow are convoluted because clouds do not allow us to see the snow and snow could potentially be flagged as clouds.

4 Discussion

We used discrete Fourier time-series to create monthly true-color images and NDVI maps at 500-m spatial resolution for 2004. The BMNG dataset is different from previous cloud-free visualizations of Earth in that it shows seasonal variations of the land surface. The high revisiting frequency of the MODIS sensor and novel atmospheric correction and cloud masking algorithms used in MODIS land products are important for producing seamless composites. However, while the Fourier adjustment of snow-free reflectance data uses sound assumptions based on seasonal phenology, compositing snow reflectances on a monthly interval presents a major difficulty in this study. A solution to this problem may be the availability of a more sophisticated snow mask, the compositing of multiple years (snow climatology), or the rejection of short-term (e.g. less than 3-4 months) snow cover data.

Figure 3 displays the two seasonal opposites January and July in 20° (It is available at 0.004667°) resolution. The algorithm we used efficiently removes cloud contamination in tropical areas. Boreal forest albedo in northern latitudes is low during winter time, since the trees project out of the snow layer [Betts and Ball, 1997], contrasted by the very high albedo of short vegetation in these areas. The brownish surface during dry season (January) in northern India and China change into dark green during the monsoon season (July). These, among many other interesting features, can be discovered while exploring the dataset. We especially encourage its application in formal and informal education. NASA is publicly sharing the BMNG dataset at no cost: (website available soon).

5 Dataset User's manual

5.1 Map projection

The BMNG dataset is gridded at the following spatial resolutions: 15, 60 and 240 arc-seconds (500m, 2km, and 8km approximate spacing at the equator). It uses a geographic (Plate Carrée) projection, which is based on an equal latitude-longitude grid spacing (not an equal area projection!). The projection datum is WGS84.

5.2 Data format

All data are available as monthly global composite images. The highest resolution at 500m is furthermore split into 8 global tiles according to Figure 4 to facilitate their handling on less powerful computer systems.

In Table 2 the file and directory structure of the BMNG dataset is outlined. The geographical extent of each global composite or tile is specified in the columns showing the upper left and the lower right edges. File suffix [Y] shows the file format: *png* (lossless compression) or *jpg* (lossy compression with quality setting

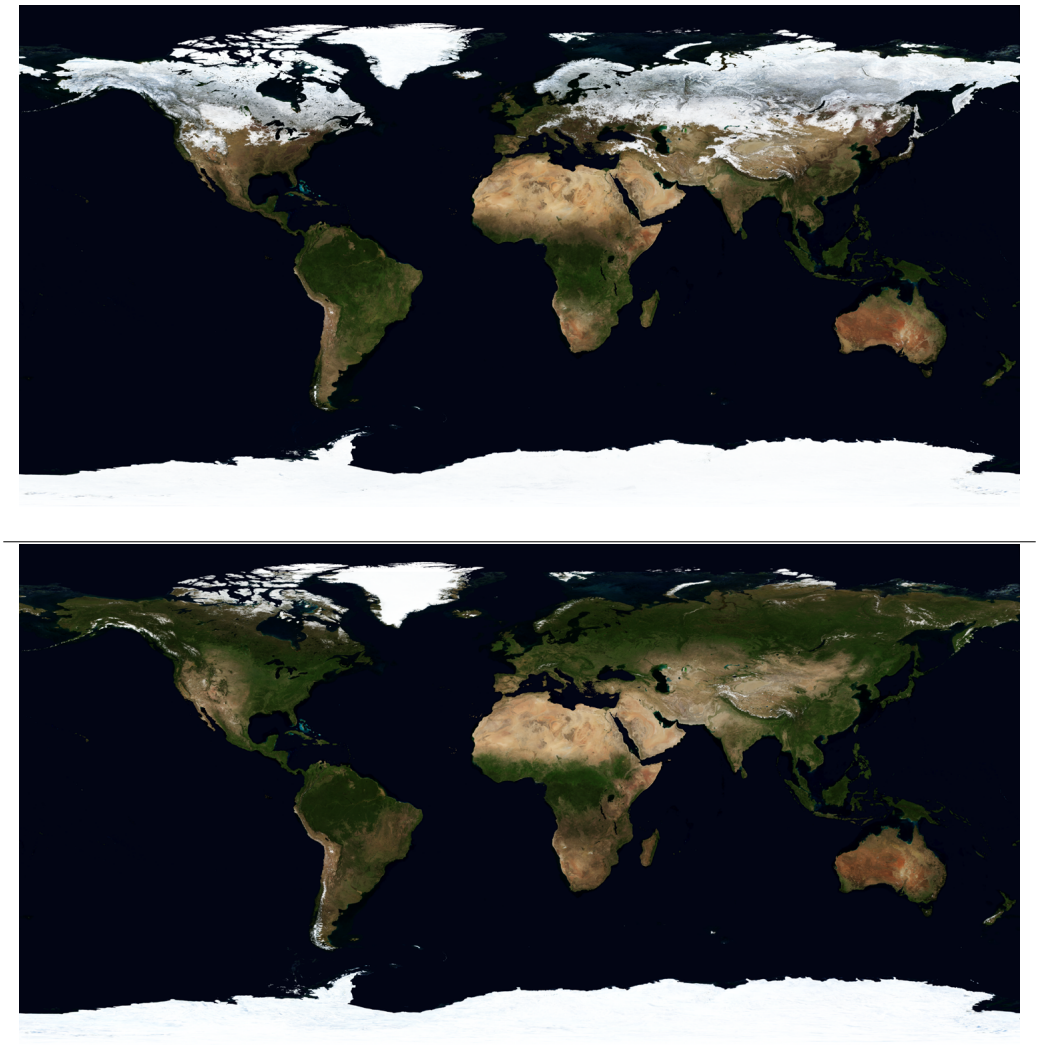

Figure 3: The Blue Marble Next Generation: true-color, cloud-free composites during January (top) and July (bottom) 2004

of 75%) [1]. The NDVI data is processed but not yet stitched on global scale. Files with monthly NDVI will be added to the BMNG dataset at a later stage.

5.3 Relief shading

The file prefix [X] is either *world* for non-shaded data, *world.topo* for a relief shading based on land topography or *world.topo.bathy* when a relief shading of land topography and ocean bathymetry was applied. The following topographic datasets were used for relief shading:

1. 3 arc-second SRTM dataset (Shuttle Radar Topography Mission, [JPL, 2005]) from 60S-60N

2. 30 arc-second GTOPO30 dataset [USGS, 1996], from 60N-90N, and to fill small voids in the SRTM dataset, using bi-cubic interpolation (David Gil,

[1] the global 500m composites stored in the *world_big* directory are raw binary files with the dimensions 3 x 86400 x 43200 (channels x columns x rows); data type is unsigned byte, with no header. They can be used for direct file access by data processing software (e.g. for subsetting, web-streaming etc.)

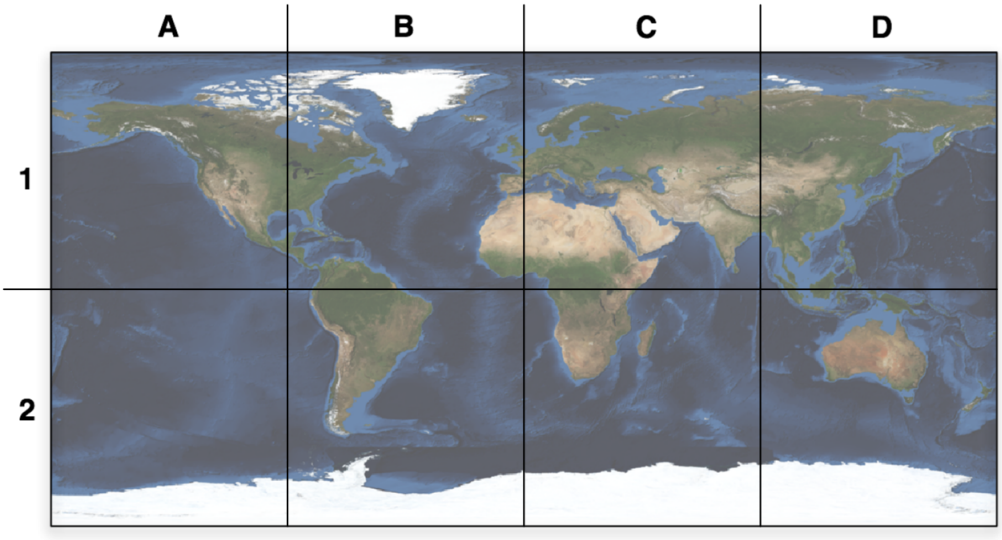

Figure 4: Sub-domains of the 500m BMNG files

Table 2: Geographic extents of the BMNG files

Directory	Filename	Upper left	Lower right	Resol. [pixels/°]
world_500m	[X].3x21600x21600.A1.[Y]	90N 180W	0N 90W	240
	[X].3x21600x21600.B1.[Y]	90N 90W	0N 0W	240
	[X].3x21600x21600.C1.[Y]	90N 0W	0N 90E	240
	[X].3x21600x21600.D1.[Y]	90N 90E	0N 180E	240
	[X].3x21600x21600.A2.[Y]	0N 180W	90S 90W	240
	[X].3x21600x21600.B2.[Y]	0N 90W	90S 0W	240
	[X].3x21600x21600.C2.[Y]	0N 0W	90S 90E	240
	[X].3x21600x21600.D2.[Y]	0N 90E	90S 180E	240
world_big	[X].3x86400x43200.bin.gz	180W 90N	180E 90S	240
world_2km	[X].3x21600x10800.[Y]	180W 90N	180E 90S	60
world_8km	[X].3x5400x2700.[Y]	180W 90N	180E 90S	15

personal communication)

3. RAMP II dataset (Radarsat Antarctic Mapping Project Digital Elevation Model Version 2, [Liu et al., 2001]) from 90S-60S

4. 1 arc-minute GEBCO (General Bathymetric Chart of the Oceans [IOC et al., 2003]) dataset

5.4 Caveats

As with digital satellite remote sensing datasets, users of the BMNG must be aware that certain characteristics of the data and artifacts of the used processing methodology may render it unsuitable for certain applications. A number of problems may be encountered by using the data:

- **Spatial accuracy:** The used MOD09A1 product is derived by reprojecting

satellite swath L1b granules into the sinusoidal projection. The BMNG is then reprojected into the geographic projection. The two involved reprojection steps may introduce small inaccuracies, and the chosen geographic projection of the final images results in distorted (smeared) appearance of higher latitude areas, since it is not an equal-area projection.

- **Temporal accuracy:** Water areas don't currently show any seasonal variation. This may be changed in future versions of the BMNG. Seasonal variations may be suppressed where heavy cloud cover does not provide sufficient temporal information. Agricultural landscapes do not necessarily follow the the continuous seasonal variations, on which our methodology is based. Apart from the climate, humans are an important driver of the plant phenology in such areas.

- **Processing artifacts:** As described in the Methods section, incomplete cloud or snow masking and problems in the atmospheric corrections in the MOD09A1 data presents a significant challenge to the extraction of monthly cloud-free land surface reflectances. The use of discrete Fourier series can remove most of these effects, but it can fail in some areas. These are especially areas with short term changes in snow cover and water, where sunglint, aerosols and other effects do not allow a good atmospheric correction of satellite reflectances.

5.5 Citation of the BMNG

R. Stöckli, E. Vermote, N. Saleous, R. Simmon and D. Herring (2005). The Blue Marble Next Generation - A true color earth dataset including seasonal dynamics from MODIS. Published by the NASA Earth Observatory. Corresponding author: rstockli@climate.gsfc.nasa.gov

6 Acknowledgements

Special thanks go to the MODIS Science Team and the MODIS Science Data Support Team for collecting, processing, and providing the MOD09A1 and the MOD12Q1 data. The present study is dependent on these science data products. System administration by John Hord, Scott Sinno and Bill Ridgway is acknowledged and much appreciated. This project is funded by NASA contract No. NAS5-01070, Task No. 4a, as a sub-contract issued by SSAI (Science Systems and Applications Inc.), sub-contract No. 2101-03-002.

References

A. K. Betts and J. H. Ball. Albedo over the boreal forest. *J. Geophys. Res.-Atmos.*, 102:28901–28909, 1997.

I. Csiszar and G. Gutman. Mapping global land surface albedo from NOAA AVHRR. *J. Geophys. Res.-Atmos.*, 104:6215–6228, 1999.

M. A. Friedl, D. K. McIver, J. C. F. Hodges, X. Y. Zhang, D. Muchoney, A. H. Strahler, C. E. Woodcock, S. Gopal, A. Schneider, A. Cooper, A. Baccini, F. Gao, and C. Schaaf. Global land cover mapping from MODIS: algorithms and early results. *Remote Sens. Environ.*, 83:287–302, 2002.

B. N. Holben. Characteristics of maximum-value composite images from temporal AVHRR data. *Int. J. Remote Sens.*, 7:1417–1434, 1986.

IOC, IHO, and BODC. Centenary edition of the gebco digital atlas. Digital Media, 2003.

M. E. James and S. N. V. Kalluri. The pathfinder AVHRR land data set - an improved coarse resolution data set for terrestrial monitoring. *Int. J. Remote Sens.*, 15:3347–3363, 1994.

JPL. Shuttle radar topography mission, 2005. URL `http://www2.jpl.nasa.gov/srtm/`.

C. O. Justice, J. R. G. Townshend, E. F. Vermote, E. Masuoka, R. E. Wolfe, N. Saleous, D. P. Roy, and J. T. Morisette. An overview of MODIS Land data processing and product status. *Remote Sens. Environ.*, 83:3–15, 2002.

Y. J. Kaufman, D. D. Herring, K. J. Ranson, and G. J. Collatz. Earth Observing System AM1 mission to earth. *IEEE Trans. Geosci. Remote Sensing*, 36:1045–1055, 1998.

H. Liu, K. Jezek, B. Li, and Z. Zhao. Radarsat antarctic mapping project digital elevation model version 2. Digital Media, 2001.

S. O. Los, G. J. Collatz, P. J. Sellers, C. M. Malmstrom, N. H. Pollack, R. S. DeFries, L. Bounoua, M. T. Parris, C. J. Tucker, and D. A. Dazlich. A global 9-yr biophysical land surface dataset from NOAA AVHRR data. *J. Hydrometeorol.*, 1:183–199, 2000.

E. G. Moody, M. D. King, S. Platnick, C. B. Schaaf, and F. Gao. Spatially complete global spectral surface albedos: value-added datasets derived from terra modis land products. *IEEE Trans. Geosci. Remote Sensing*, 43(1):144–158, 2005.

S. Moulin, L. Kergoat, N. Viovy, and G. Dedieu. Global-scale assessment of vegetation phenology using NOAA/AVHRR satellite measurements. *J. Clim.*, 10:1154–1170, 1997.

S. W. Running, D. D. Baldocchi, D. P. Turner, S. T. Gower, P. S. Bakwin, and K. A. Hibbard. A global terrestrial monitoring network integrating tower fluxes, flask sampling, ecosystem modeling and eos satellite data. *Remote Sens. Environ.*, 70:108–127, 1999.

R. Stöckli and P. L. Vidale. European plant phenology and climate as seen in a 20-year AVHRR land-surface parameter dataset. *Int. J. Remote Sens.*, 25(17): 3303–3330, 2004.

R. Stöckli, A. Nelson, and F. Hasler. The blue marble, 2000. URL `http://rsd.gsfc.nasa.gov/rsd/bluemarble/bluemarble2000.html`.

R. Stöckli, R. Simmon, and D. Herring. The MODIS blue marble, 2002. URL `http://earthobservatory.nasa.gov/Newsroom/BlueMarble/`.

N. Tholey. Digital processing of Earth observation images. *Surveys In Geophysics*, 21:209–222, 2000.

USGS. GTOPO30. Digital Media, 1996. URL `http://edcdaac.usgs.gov:80/gtopo30/gtopo30.html`.

E. F. Vermote, N. ElSaleous, C. O. Justice, Y. J. Kaufman, J. L. Privette, L. Remer, J. C. Roger, and D. Tanre. Atmospheric correction of visible to middle-infrared EOS-MODIS data over land surfaces: Background, operational algorithm and validation. *J. Geophys. Res.-Atmos.*, 102:17131–17141, 1997.

E. F. Vermote, N. Z. El Saleous, and C. O. Justice. Atmospheric correction of MODIS data in the visible to middle infrared: first results. *Remote Sens. Environ.*, 83:97–111, 2002.

B. A. Wielicki, R. D. Cess, M. D. King, D. A. Randall, and E. F. Harrison. Mission to planet earth - role of clouds and radiation in climate. *Bulletin Am. Meteorol. Soc.*, 76:2125–2153, 1995.